Electronic Supplementary Information

C-supported WO$_x$-Ru based Catalysts for the Selective Hydrogenolysis of Glycerol to 1,2-Propanediol

Alessandro Bellè,[a] Kohei Kusada,[b] Hiroshi Kitagawa,[b] Alvise Perosa,[a] Lidia Castoldi, Daniele Polidoro, and Maurizio Selva*[a]

[a] Dipartimento di Scienze Molecolari e Nanosistemi dell'Università Ca' Foscari Venezia,

Via Torino, 155 – 30175, Venezia Mestre (Italy)

[b] Graduate School of Science, Kyoto University, Yoshida-honmachi, Sakyo-ku, Kyoto

606-8501 Japan

Email: selva@unive.it

List of contents

The preparation of the catalysts. Catalysts were prepared via three procedures: i) co-impregnation of the metal components on C; ii) impregnation of W con C followed by the subsequent introduction of Ru component; iii) mechanical mixing.

i) Co-impregnation. was carried out by the following procedure. A suspension of carbon (NORIT SX 1G; 1 g), $RuCl_3$ (0.5 mmol), Na_2WO_4 (0.03-0.5 mmol), and water (40 mL) was stirred for 2 hours at rt, added with conc.d aq. HCl (0.5 mL; 37 wt%), and heated at 80 °C for 3 h. After the removal of water under vacuum, the solid was dried (180 °C overnight, under a N_2 flow of 20 mL/min) and reduced at 300 °C (H_2: 25 mL/min, 3 h). Scheme S1 reports the expected reactions.

$$Na_2WO_4 + 2HCl \longrightarrow WO_3{*}H_2O + 2NaCl$$

$$RuCl_3{*}H_2O \xrightarrow{H_2} Ru(0) + HCl + H_2O$$

$$WO_3{*}H_2O + H_2 \xrightarrow{Ru\,/\,H_2} WO_x$$
$$H_2O$$
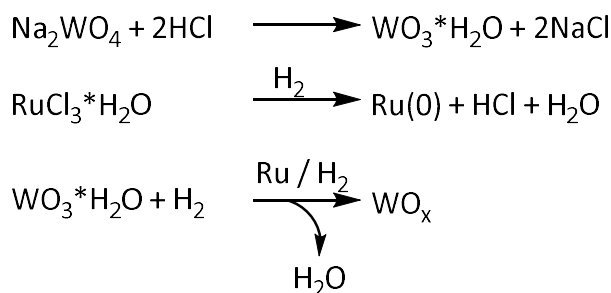
Scheme S1. Expected reactions during the co-impregnation of $RuCl_3$ and Na_2WO_4 precursors.

HCl allowed the decomposition of the sodium tungstate, and the strong acidity prevented the re-dissolution of WO_3 species. The collected powder was finally washed with milli-Q water (50 mL), filtered, dried, and stored.

ii) Impregnation of W con C followed by the subsequent introduction of Ru. Na_2WO_4 (1 mmol) was impregnated on carbon black powder (NORIT SX 1G; 1 g) according to the above described procedure (water: 40 mL; conc.d aq. HCl: 0.5 mL, 37 wt%; 80 °C, 3 h; water distillation, drying at 180 °C with N_2, reduction at 300 °C in H_2, and final washing with water). The expected amount of W on C was 2 wt%. The solid sample was labelled as $2WO_x/C$. This was used as a support to introduce the second metal component, Ru, either through a subsequent impregnation carried out as follows. A suspension of $RuCl_3{\cdot}H_2O$ (105 mg, 0.5 mmol) and $2WO_x/C$ (1 g) in water (40 mL) was stirred for 2 hours at rt, added with conc.d aq. HCl (0.5 mL; 37 wt%), and heated at 80 °C for 3 h. Then, drying, reduction and washing were carried out with the same protocol used above for co-impregnated catalysts. The expected Ru:W molar ratio in the sample was of 4. This catalyst was labelled as $[Ru-2WO_x/C]_{ts}$ (ts=two-step synthesis).

iii) Mechanical mixing. At rt, a solid sample was obtained by mixing $2WO_x/C$ (150 mg) and commercial 5% Ru/C (150 mg) in a mortar. This catalyst was labelled as $[Ru-2WO_x/C]_{mm}$ (mm=mechanical mixture): the corresponding loadings of the metal components were 2.5 and 1 wt% for Ru and W, respectively.

ICP analyses of catalytic samples. ICP-OES analysis were run using a Perkin Elmer Optima 5300DV. A calibration curve was obtained by using twelve aqueous solutions of containing 0, 100, 200, 300, 500, 1000, 2000, 3000, 4000, 5000, 6000, 7000 ppb of each targeted element (Ru, W, and Na). These solutions were prepared by dilution of a 1000 mg/L standard calibration solution of $RuCl_3$ in HCl, $(NH_4)_2WO_4$ in H_2O and NaCl in H_2O. The linear fit of Ru, W and Na were automatically calculated by the ICP software resulting with interceptors of -1156.0, -729.2 and -13,3, slopes of 22.08, 26.36 and 0.617, and correlation coefficients of 0.999897, 0.999972 and 0.999883, respectively.

ICP analyses were carried out to determine the metal loading on the solid catalysts after their synthesis (Table 1). The solids were digested in the presence of a highly oxidants solution under MW irradiation. In a typical procedure, a selected sample (50 mg) was charged into a PTFE vessel (bomb) with aqua regia (4 mL) and H_2O_2 (2 mL, 30 v/v%). The bombs were placed in a microwave oven (MILESTONE "ETHOS 1600") and the following power ramp was set: i) 400 W for 2 min; ii) 250 W for 4 min; iii) 400 W for 4 min; iv) 600 W for 8 min. At the end of the digestion step, a homogeneous solution was obtained. This was transferred in 50 mL graduated flask and brought to volume with milli-Q water. The prepared solution (1 mL) was further diluted with milli-Q water (9 mL), and finally analyzed. Analyses were run in axial direction at 240.272, 207.912 and 589.592 nm for Ru, W, and Na, respectively. The contents of Ru, W and Na recorded for each analysis were the average of 6 subsequent acquisitions.

Preliminary screening of the hydrogenolysis of glycerol with a commercial 5% Ru/C. Experiments were carried out in a stainless-steel autoclave, using an aq. glycerol solution (10 mL, 10% w/w), 5% Ru/C (150 mg, 0.075 mmol of Ru), gaseous H_2 (60 bar), and by changing the time and the temperature between 5 and 25 hours, and 120 and 190 °C, respectively.
The reaction provided several liquid and gaseous products (Scheme S2).

Others

MeOH, EtOH, CH_4, CO, CO_2, etc

1,2-PDO **EG**
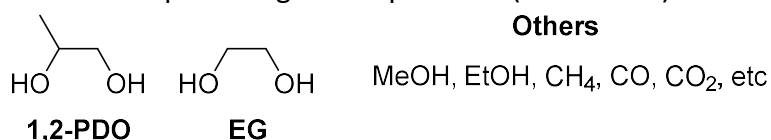
Scheme S2. Products observed in the hydrogenolysis of glycerol at different T, p and reaction time

The attention was placed on liquid derivatives as 1,2-PDO and EG (1,2-propanediol and ethylene glycol). The formation of these two compounds and the conversion of glycerol were determined by GC using triglyme as an external standard. Other products, named as "others", included light liquids (mostly methanol and ethanol) and gases (mostly CO, CO_2, and CH_4) whose total amount was the complement to 100 of the overall reaction selectivity. The structure of products was assigned by GC/MS.
Figure S1 reports the results of experiments performed at 60 bar for 12 hours, in the range of 120-190 °C.
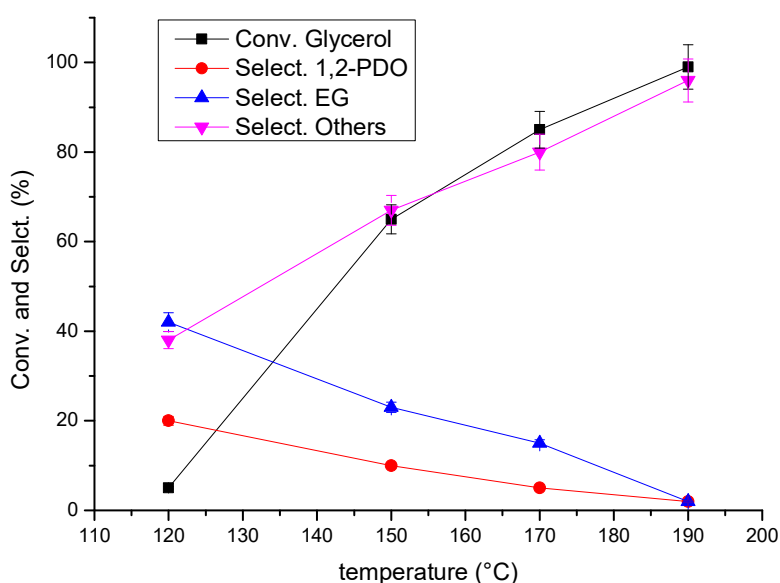
Figure S1. Effect of the temperature on the catalytic hydrogenolysis of glycerol carried out at 60 bar (H_2), for 12 hours, using an aqueous solution of glycerol (10 mL, 10% w/w) and Ru/C (150 mg, 5 wt%). Conversion of glycerol over time

(black profile). Red and blue: selectivity to 1,2-PDO and EG, respectively. Magenta: "others" as the sum of light liquid products (mostly MeOH and EtOH) and gases (mostly CO, CO_2, and CH_4), other than 1,2-PDO and EG.

C-C bond cleavage reactions were favored over the desired formation of 1,2-PDO even at a moderate temperature: at 120 °C, although the conversion of glycerol was as low as 5%, major products were EG (42%) and "others" (38%), while the selectivity towards 1,2-PDO was only 20%. As the temperature was raised progressively to 190 °C, the conversion increased to a quantitative value along with the predominant formation of light liquids and gaseous derivatives ("others"). Only traces of 1,2-PDO and EG were observed. From these results, the study was continued at 150 °C for 12 hours, under conditions by which a reasonably good conversion (70%) was reached and the total selectivity of PDO and EG (12+26=38%) was not far from that corresponding to the sum of all other products ("others", 62%).

Figure S2 reports the effect of the reaction time for the reaction performed at 150 °C and 60 bar.
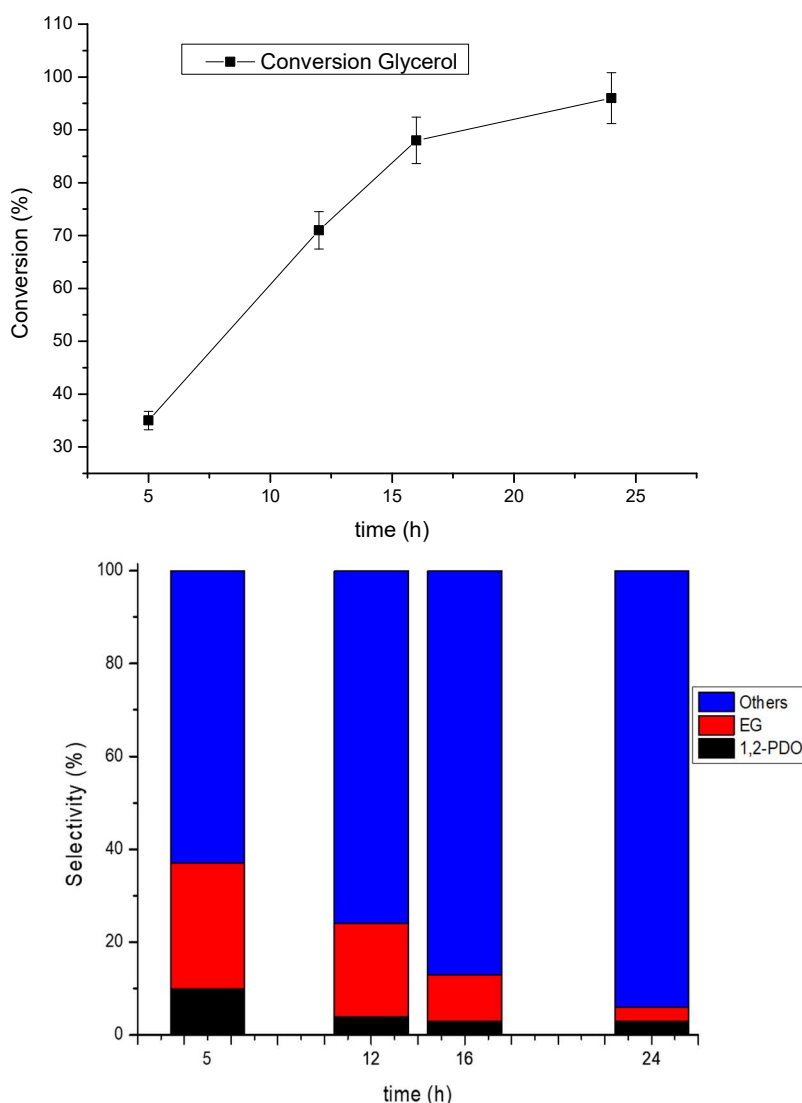
Figure S2. Effect of the reaction time on the catalytic hydrogenolysis of glycerol carried out at 150 °C and 60 bar (H_2), using an aqueous solution of glycerol (10 mL, 10% w/w) and Ru/C (150 mg, 5 wt%). Top: conversion of glycerol over time. Bottom: products distribution. Black and red bars: 1,2-PDO and EG. Blue bar, "others", was the sum of light liquid products (mostly MeOH and EtOH) and gases (mostly CO, CO_2, and CH_4), other than PDO and EG.

The glycerol conversion smoothly increased from 35% up to almost quantitative by increasing the reaction time from 5 to 14 hours, respectively (top). The products distribution, however, was rather unsatisfactory with a maximum selectivity towards 1,2-PDO and EG not exceeding 10 and 27%, respectively, achieved at low conversion (bottom left: red and black bars). As the reaction time was increased and the reaction proceeded further, the formation of both EG and 1,2-PDO was negligible (≤5% each) and the majority of products came from competitive C-C bond cleavage processes (blue bar). This behavior was in agreement with previous studies reporting that the (low) density of acid groups on Ru/C was not enough for an efficient activation of the dehydration step required for the selective formation of 1,2-PDO.[1]

Effect of the glycerol concentration in the hydrogenolysis of glycerol catalyzed by Ru-2WOₓ/C. A set of experiments was carried out to explore the effect of the concentration of glycerol using aqueous solutions in the range of 5 to 20 wt%. The H_2 pressure (5 bar), the temperature (150 °C) and time (12 h), the catalyst (Ru-2WOₓ/C, 150 mg) and the overall volume of the aqueous solution (5 mL) in each run were kept unchanged with respect to the optimization study from Figure 1. Results are reported in Figure S3 which illustrates the trend of the conversion and the 1,2-PDO selectivity as a function of the glycerol concentration.

The concentration of glycerol remarkably affected the extent of its hydrogenolysis. The conversion decreased from quantitative to 67, 48, 31, and 18% as the reactant solution was progressively concentrated from 5 to 20 wt. %, while the 1,2-PDO selectivity was improved from 88 to > 95% (red profile). Since by-products were mixtures of ethylene glycols and light alcohols (C1-C3) deriving from both C-C bond cleavage reactions and dehydration/hydrogenation of 1,2-PDO (paths 1 and 2, Scheme 1), Figure S3 suggested that such mechanisms could be tuned by the amount of glycerol adsorbed onto the catalytic surface, *i.e.* by varying the concentration of the reacting solution. This control of the products distribution confirmed the trend of Figure 1 and was in agreement with previously reported results: for example, in the hydrogenolysis of glycerol catalyzed by a bimetallic PtRu/C system, the selectivity towards 1,2-PDO was reported to improve from 18 to 30% when the conversion decreased from quantitative to 23%.[1]
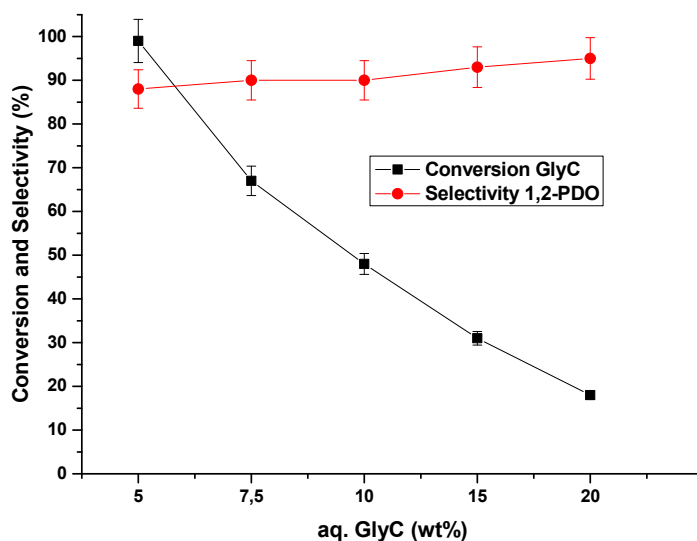
Figure S3. The hydrogenolysis of GlyC carried out over Ru-2WOₓ/C (150 mg) at different concentrations of the aqueous solution (5 mL) of GlyC. Other conditions: 150 °C, 5 bar (H_2), 12 hours.

Recycle of Ru-2WO$_x$/C. in addition to experiments described in Figure 2, the catalyst stability was further investigated by a second set of recycle tests. Reactions and recycles were carried under the same conditions of Figure 2, except for the H$_2$ pressure and the reaction time which were both increased up to 35 bar and 12 hours, respectively. Results are illustrated in Figure S4 which shows the trend of the glycerol conversion and the products distribution in five subsequent runs.
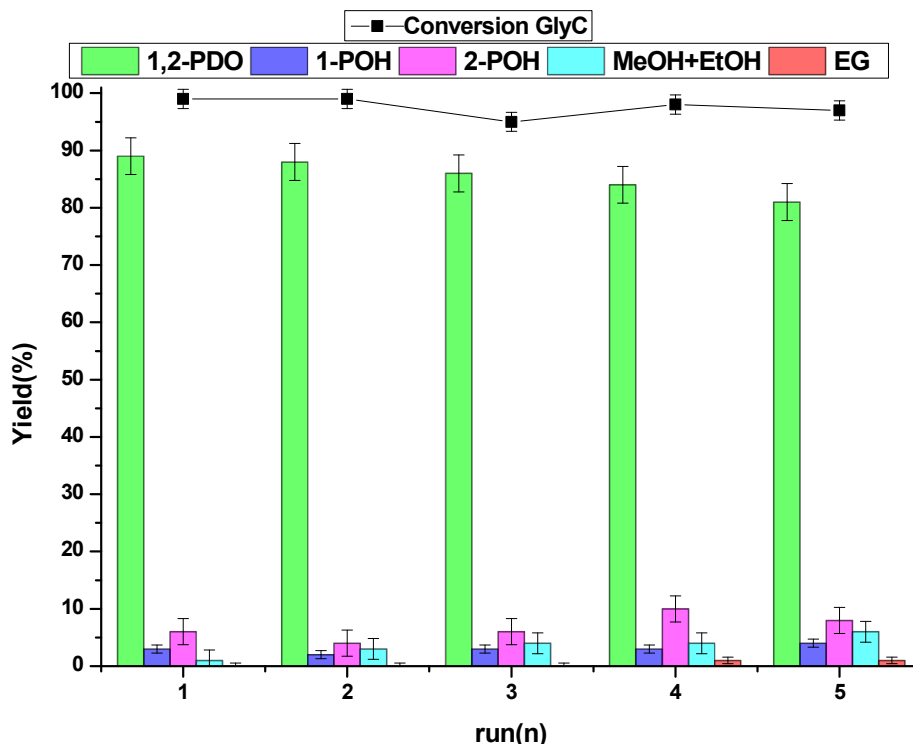
Figure S4. Recycle tests of Ru-2WO$_x$/C (150 mg). Reaction conditions: aq. solution of glycerol (5 mL, 5 wt%), 150 °C, 35 bar of H$_2$ bar, 12 h.

Notwithstanding the (moderate) leaching of W, recycle tests showed that the performance of the catalyst was stable enough over time. The combination of a high pressure and prolonged reaction time allowed a quantitative conversion of glycerol which did not substantially change during all experiments. The 1,2-PDO selectivity showed instead, a gradual slight decrease from 88 to 82% (green bars) plausibly due to multiple effects of pressure on the H$_2$ solubility in water,[2] and over-reduction of W(VI) species resulting in a decrease of the catalyst acidity (see also comments to Figure 1 , right).[3]

Characterization of the catalysts. WO$_x$-modified Ru catalysts supported on C were characterized by XPS, TEM, XRF and XRD to investigate their morphological-structural properties.
XPS analysis. X-ray photoelectron spectroscopy (XPS) was performed using a Perkin Elmer Φ 5600ci spectrometer using nonmonochromatic Al Kα radiation (1486.6 eV) in the 10^{-7} Pa pressure range. All the binding energy (BE) values are referred to the Fermi level. The correct calibration of the BE scale was verified by checking the position of both Ru3p$_{3/2}$ and W4f$_{7/2}$ bands (from pure metal targets). After a Shirley-type background subtraction, the raw spectra were fitted using a nonlinear least-squares fitting program adopting Gaussian−Lorentzian peak shapes for all the peaks. Standard energy differences between the different tungsten oxides and ruthenium species were considered in the curve filling process of the Ru3p and W4f energy region of the systems studied in this work. Samples did not show surface charging during analysis; however, due to the large amount of C with respect to Ru (the C/Ru ratio is around 20), only the Ru3p doublet band was recorded, while the

Ru3d band was overlapped by the much more intense C1s band. The uncertainty of the determined BEs was lower than 0.2 eV. The atomic composition was evaluated using sensitivity factors as provided by Φ V5.4A software. The relative uncertainty of the reported atomic fraction of the different elements is lower than 0.1.

XPS analyses were carried out for the best performant catalyst used in the hydrogenolysis of glycerol, Ru-2WO$_x$/C. This was characterised before and after its use and its properties were compared to those of the sample containing only W, 2WO$_x$/C (see Table 1 for sample labels).

Figures S5, S6 and S7 report the XPS spectra of fresh and used Ru-2WO$_3$/C and 2WO$_x$/C, respectively. Binding energies are reported within an experimental error of + 0.2 eV.
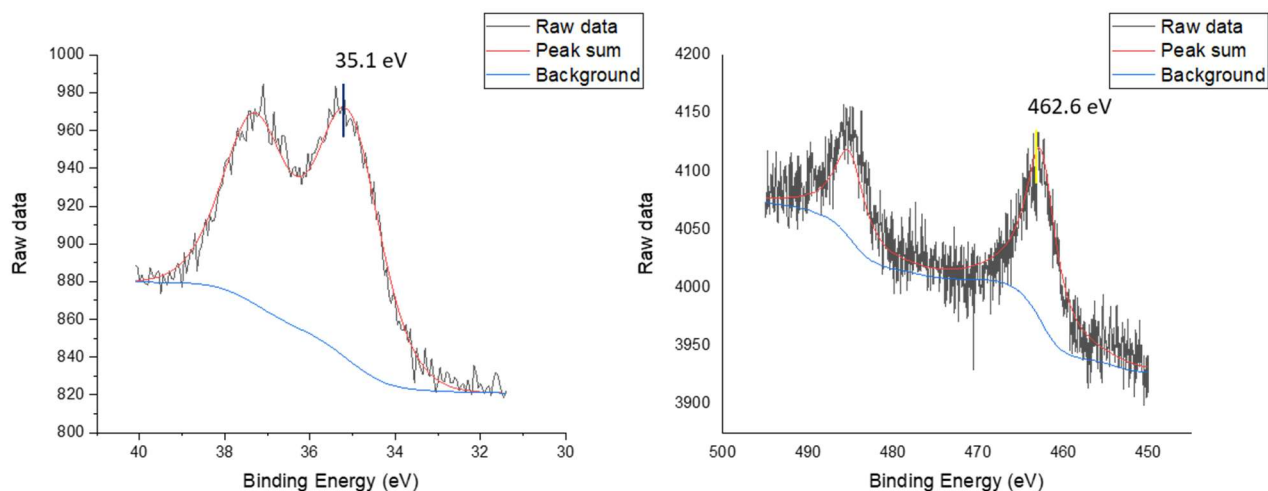
Figure S5. XPS spectra of fresh Ru-2WO$_3$/C. Left: binding energy of W4f; right: binding energy of Ru3p.
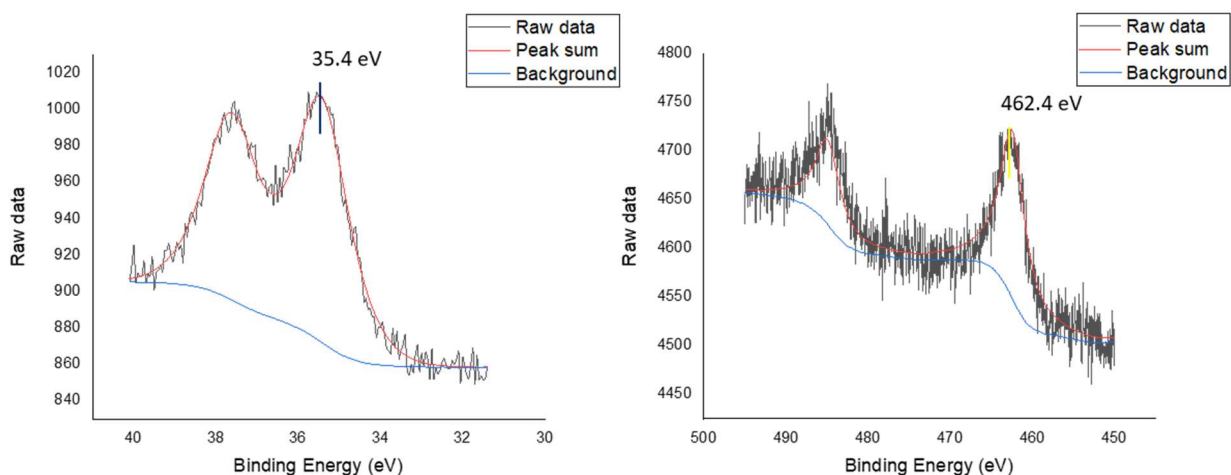
Figure S6. XPS spectra of used Ru-2WO$_3$/C. Left: binding energy of W4f; right: binding energy of Ru3p.
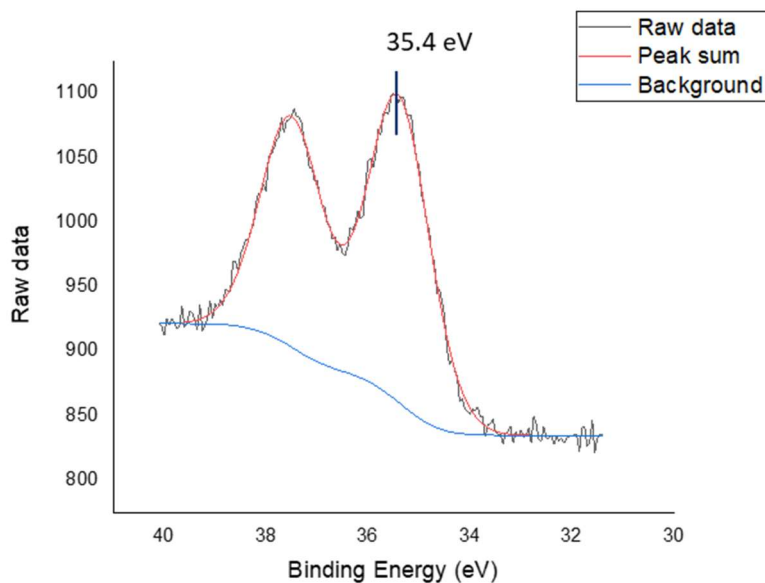
Figure S7. XPS spectrum of $2WO_x/C$: binding energy of W4f.

In the fresh Ru-$2WO_x$/C sample, the 4f doublet of tungsten showed the W4f$_{7/2}$ signal at 35.1 eV of BE and with a FWHM of 1.8 eV (Figure S5, left). The spin-orbit-splitting distance between the two doublet signals was 2.2 eV. Albeit the W4f$_{7/2}$ BE was characteristic of WO_3 and matched the literature data, [4,5] the presence of W in +5 oxidation state could not be completely excluded: the very low amount of W with respect to oxygen prevented any significant fit on the O1s band involving contributions coming different W oxides. The 3p doublet band of ruthenium showed the Ru3p$_{3/2}$ signal falling at 462.6 eV of BE and with a FWHM of 4.4 eV (Figure S5, right). The spin-orbit-splitting distance between the two doublet signals was 22.5 eV. The Ru3p$_{3/2}$ BE was consistent with the presence of Ru oxide, RuO_2.[6,7] However, since the difference in BE between oxidized and metallic species is usually limited to few tenths of eV in Ru3p$_{3/2}$ band, Ru could be present in oxidation states lower than +4. From spectra, the evaluated Ru:W molar ratio was 3.8 (averaged on 4 samples) in agreement with the expected value of 4 and the ICP analyses (Table 1).

The used Ru-$2WO_x$/C sample was the catalyst recovered after the hydrogenolysis of glycerol carried under the conditions of Figure 1 (150 °C, 5 bar, 6h). The analysis of the corresponding XPS spectra (Figure S6) did not indicate significant changes with respect to the above described XPS spectra of the fresh catalyst. The 4f doublet of tungsten showed the W4f$_{7/2}$ signal at 35.4 eV of BE and with a FWHM of 1.6 eV (Figure S6, left). The spin-orbit-splitting distance between the two doublet signals was 2.2 eV. The 3p doublet band of rutheniun showed the Ru3p$_{3/2}$ signal at 462.4 eV of BE. The FWHM of 3.7 eV (Figure S6, right) was slightly smaller than for the fresh sample, suggesting a better-defined chemical state of Ru. The spin-orbit-splitting distance between the two doublet signals was 22.5 eV. As for the fresh sample, the Ru3p$_{3/2}$ BE of the used catalyst was consistent with the presence of RuO_2, but this could not exclude that even a significant amount of Ru was in oxidation states lower than +4.

XRD analyses. XRD spectra of fresh and used Ru-2WOx/C are reported in Figure S8, left and right).
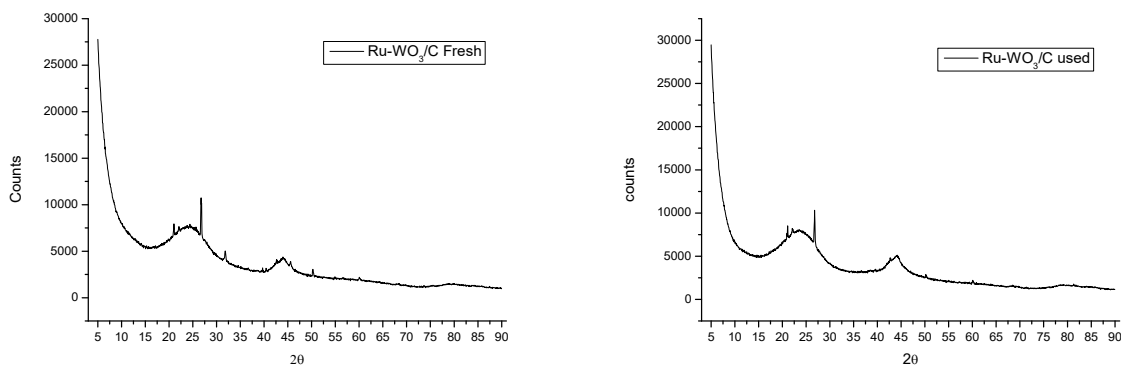
Figure S8. XRD spectra of the Ru-2WO$_3$/C sample. Left and right: fresh and used catalysts, respectively.

The diffraction profiles of both samples matched that of carbon used as a support.[8] This result was in agreement with TEM analyses that showed the presence of very small metal nanoparticles (below 2 nm) undetectable by XRD

GC calibration curves. The calibration curves were obtained by the analysis of a solution (0.4 mL) prepared by mixing an aqueous solution of diethylenglycol dimethylether [diglyme, MeO(CH$_2$CH$_2$O)$_2$Me; 0.2 mL, 0.01 M) as a standard, and an appropriate amount (0.2-0.02 mL) of an aqueous solution of the desired substrate.
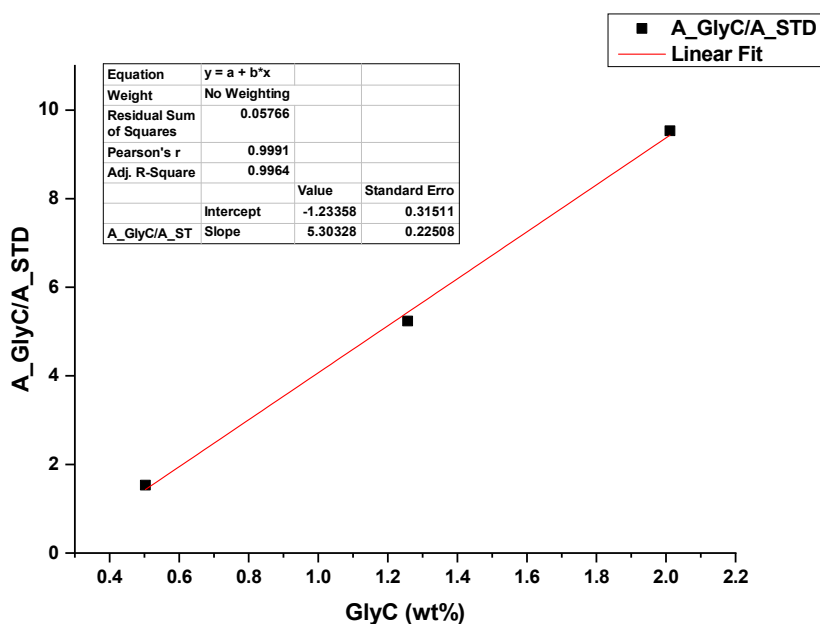
Figure S9. GC calibration curve for glycerol obtained using triethylenglycol dimethylether as an external standard
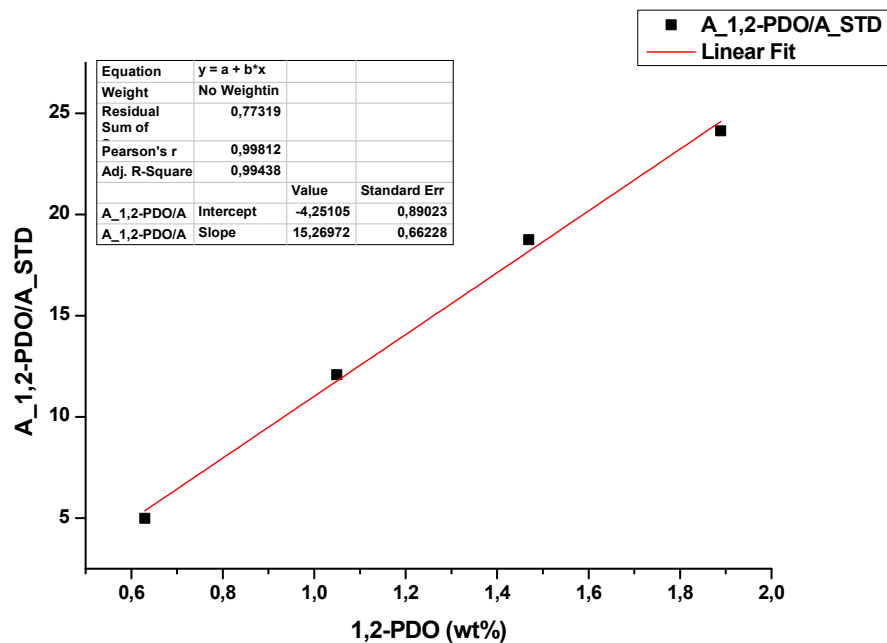
Figure S10. GC calibration curve for 1,2-propanediol (1,2-PDO) obtained using triethylenglycol dimethylether as an external standard
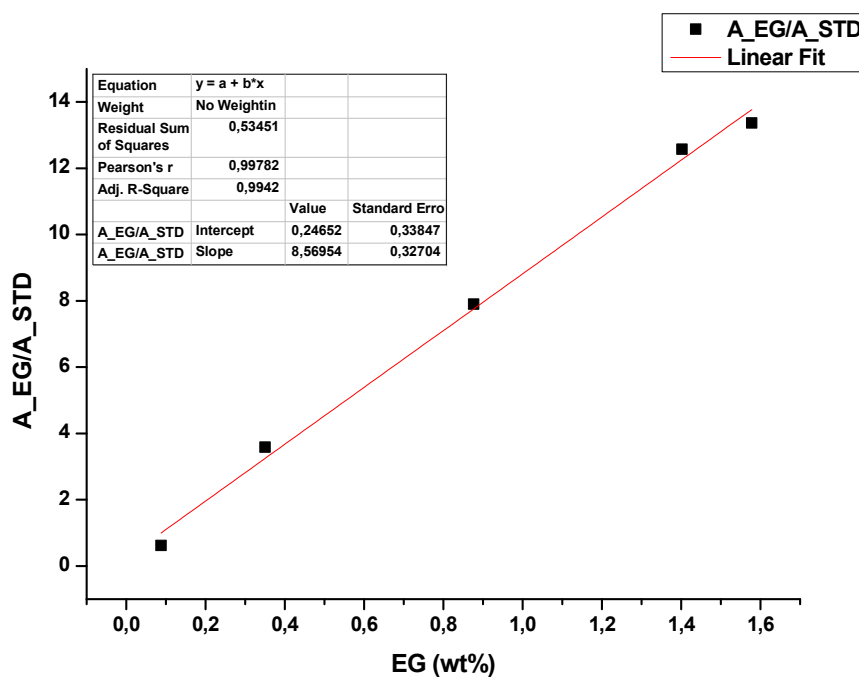
Figure S11. GC calibration curve for ethylene glycol (1,2-PDO) obtained using triethylenglycol dimethylether as an external standard

Equation	y = a + b*x		
Weight	No Weighting		
Residual Sum of Squares	0.10968		
Pearson's r	0.99991		
Adj. R-Square	0.99963		
		Value	Standard Erro
A_2-POH/A_STD	Intercept	0.48832	0.31914
	Slope	46.27946	0.63002
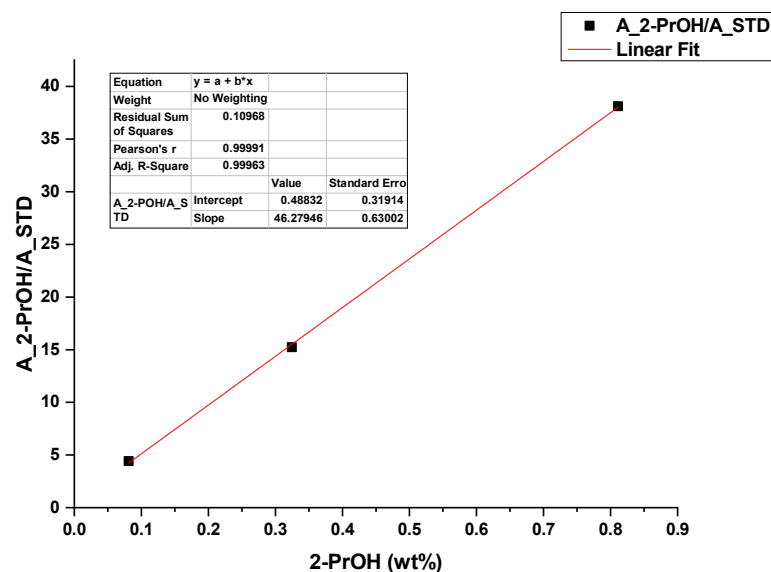
Figure S12. GC calibration curve for 2-PrOH obtained using triethylenglycol dimethylether as an external standard

Equation	y = a + b*x		
Weight	No Weightin		
Residual Sum of	1,87336		
Pearson's r	0,99768		
Adj. R-Square	0,99304		
		Value	Standard Err
A_EtOH/A_ST	Intercept	0,60269	0,67156
A_EtOH/A_ST	Slope	42,44156	2,04955
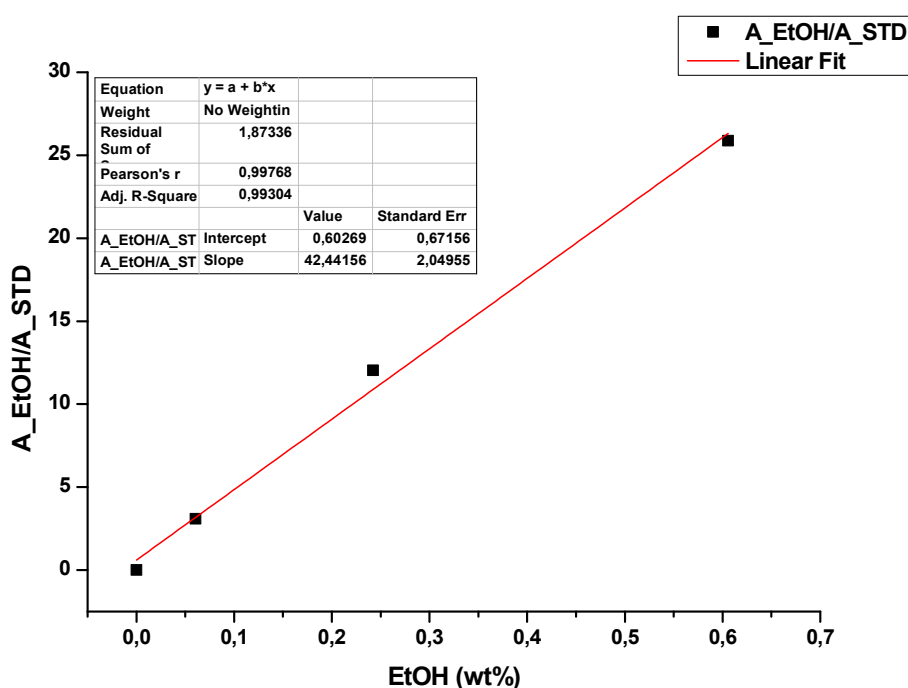
Figure S13. GC calibration curve for ethanol obtained using triethylenglycol dimethylether as an external standard

CO chemisorption. The CO chemisorption measurements are often used to determine the metal particle size. The relationship between the metal dispersion (D) and the mean particle size (d_{Ru}) is defined as:

$$D_{Ru} = 6 \frac{\left(v_m / a_m \right)}{d_{Ru}}$$

In the case of Ru with a hcp structure the area occupied by a surface atom (a_m) is 6.35 Å^2 while the volume occupied by an atom in bulk metal (v_m) is 13.65 Å^3. Accordingly, Table S1 reports the Ru

dispersion and the Ru particle size calculated for the three investigated catalysts, Ru-2WO$_x$/C, Ru-1WO$_x$/C and Ru-0.5WO$_x$/C, respectively.

Table S1. The Ru dispersion and the Ru particle size calculated from CO chemisorption measurements

Entry	Sample	Ru:W (molar ratio)	Tot. CO ads [µmol/g]	D$_{Ru}$ (%)	d$_{Ru}$ (nm)[9]
1	Ru2WO$_x$/C	4:1	35	7	18
2	Ru1WO$_x$/C	8:1	70	14	9
3	Ru0.5WO$_x$/C	16:1	77	15	8

However, in the case of the bimetallic Ru/W systems studied in this work, it should be noted that the CO adsorption could involve both metals, not only Ru, but also W in its oxide form (WO$_x$). Indeed, during the thermal desorption (TPD) carried out during the CO-chemisorption tests, two desorption peaks were noticed. Moreover, the intensity of the second peak increased by increasing the WO$_x$ loading on the catalyst. These observations:
  i)   were consistent with the attribution of the first and the second peak to CO desorbed from Ru (at a lower temperature) and from WO$_x$, respectively.
  ii)   could plausibly explain the discrepancy on the Ru particle size measured by TEM (ca 1. 5 nm) and by CO chemisorption (18 nm) for the same Ru2WO$_x$/C catalyst.
In light of this, the size of Ru particles determined by TEM (averaged on more than 100 metal nanoparticles) was considered a more reliable measure than that achieved from CO chemisorption.

References

[1] E. P. Maris, W. C. Ketchie, M. Murayama, R. J. Davis *J. Catal.* **2007**, *251*, 281–294.

[2] H. A. Pray, C. E. Schweickert, B. H. Minnich *Ind. Eng. Chem.* **1952**, *44*, 1146–1151.

[3] A. Alhanash, E. F. Kozhevnikova, I. V. Kozhevnikov *Catal Lett* **2008**, *120*, 307–311.

[4] N. Tammanoon, T. Iwamoto, T. Ueda, T. Hyodo, A. Wisitsoraat, C. Liewhiran, Y. Shimizu *ACS Appl Mater Interfaces* **2020**, *12*, 41728-41739.

[5] P. Charton, L. Gengembre, P. Armand, *J. Solid State Chem.* **2002**, *168*, 175–183.

[6] K. Qadir, S. H. Joo, B. S. Mun, D. R. Butcher, J. Russell Renzas, F. Aksoy, Z. Liu, G. A. Somorjai, J. Y. Park *Nano Lett.* **2012**, *12*, 5761–5768.

[7] W. Wang, Y. Li, H, Wang *React. Kinet. Mech. Catal.* **2013**, *108*, 433–441

[8] X-Y. Liu, M. Huang, H.-L. Ma, Z.-Q. Zhang, J.-M. Gao, Y.-L. Zhu, X.-J. Han, X.-Y. Guo *Molecules* **2010**, *15*, 7188-7196

[9] G. Ertl, H. Knözinger, F. Schmith, J. Weitkamp, Jens *Handbook of Heterogeneous Catalysis (Online), Particle Size and Dispersion Measurements*, Wiley-VCH, 2008